

**CO₂ dispersion
modelling over Paris**

C. Lac et al.

CO₂ dispersion modelling over Paris region within the CO₂-MEGAPARIS project

C. Lac¹, R. P. Donnelly¹, V. Masson¹, S. Pal², S. Donier¹, S. Queguiner¹,
G. Tanguy¹, L. Ammoura², and I. Xueref-Remy²

¹CNRM-GAME (CNRS-Meteo-France), URA1357, Toulouse, France

²Laboratoire des Sciences du Climat et de l'Environnement (LSCE), IPSL-UVSQ-CNRS-CEA,
Orme des Merisiers, Gif-Sur-Yvette, France

Received: 11 September 2012 – Accepted: 2 October 2012 – Published: 25 October 2012

Correspondence to: C. Lac (christine.lac@meteo.fr)

Published by Copernicus Publications on behalf of the European Geosciences Union.

Title Page

Abstract

Introduction

Conclusions

References

Tables

Figures

◀

▶

◀

▶

Back

Close

Full Screen / Esc

Printer-friendly Version

Interactive Discussion



Abstract

Accurate simulation of the spatial and temporal variability of tracer mixing ratios over urban areas is challenging, but essential in order to utilize CO₂ measurements in an atmospheric inverse framework to better estimate regional CO₂ fluxes. This study investigates the ability of a high-resolution model to simulate meteorological and CO₂ fields around Paris agglomeration, during the March field campaign of the CO₂-MEGAPARIS project. The mesoscale atmospheric model Meso-NH, running at 2 km horizontal resolution, is coupled with the Town-Energy Balance (TEB) urban canopy scheme and with the Interactions between Soil, Biosphere and Atmosphere CO₂-reactive (ISBA-A-gs) surface scheme, allowing a full interaction of CO₂ between the surface and the atmosphere. Statistical scores show a good representation of the Urban Heat Island (UHI) and urban-rural contrasts. Boundary layer heights (BLH) at urban, sub-urban and rural sites are well captured, especially the onset time of the BLH increase and its growth rate in the morning, that are essential for tall tower CO₂ observatories. Only nocturnal BLH at sub-urban sites are slightly underestimated a few nights, with a bias less than 50 m. At Eiffel tower, the observed spikes of CO₂ maxima occur every morning exactly at the time at which the Atmospheric Boundary Layer (ABL) growth reaches the measurement height. The timing of the CO₂ cycle is well captured by the model, with only small biases on CO₂ concentrations, mainly linked to the misrepresentation of anthropogenic emissions, as the Eiffel site is at the heart of traffic emission sources. At sub-urban ground stations, CO₂ measurements exhibit maxima at the beginning and at the end of each night, when the ABL is fully contracted, with a very strong spatio-temporal variability. The CO₂ cycle at these sites is generally well reproduced by the model, even if some biases on the nocturnal maxima appear in the Paris plume partly due to small errors on the vertical transport, or in the vicinity of airports due to small errors on the horizontal transport (wind direction). A sensitivity test without urban parameterisation removes UHI and underpredicts nighttime BLH over urban and sub-urban sites, leading to large overestimation of nocturnal CO₂ concentration at the sub-urban sites. The

CO₂ dispersion modelling over Paris

C. Lac et al.

Title Page

Abstract

Introduction

Conclusions

References

Tables

Figures

◀

▶

◀

▶

Back

Close

Full Screen / Esc

Printer-friendly Version

Interactive Discussion



agreement of daytime and nighttime BLH and CO₂ predictions of the reference simulation over Paris agglomeration demonstrates the potential of using the meso-scale system on urban and sub-urban area in the context of inverse modelling.

1 Introduction

It has been widely reported that atmospheric CO₂ concentration has increased by more than 30 % since the pre-industrial era mainly due to human activities and this increase is very likely at the root of the observed temperature rise of 0.6 °C over the last century (Forster et al., 2007). Although we have good estimates of the CO₂ fluxes on a global basis, and have a relatively well-established observation network to detect the largescale trends, regional information (10–500 km) is needed if society is ever to manage or verify carbon emissions (Dolman et al., 2006). We must improve our understanding of regional variations in sources and sinks of CO₂ to identify possible sequestration or emission management options. It is necessary to discriminate between the anthropogenic and biospheric sources which overlap very strongly in European countries. In this context, the project CO₂-MEGAPARIS aims at the quantification of the CO₂ emissions of the megacity Paris, and consequently the simulation and assessment of the anthropogenic CO₂ plume over the Ile-de-France province (corresponding to the Paris administrative region) (Xueref-Remy et al., 2012). Indeed, with 12 millions of inhabitants, Paris is the third megacity of Europe (after London and Moscow), emits about 14 % of national emissions. Moreover, it is an ideal location due to its relatively well defined boundaries and the lack of other major CO₂ emitters in its immediate vicinity. The former experiment ESQUIF (Vautard et al., 2003) gave a fair understanding of the atmospheric dynamics in this area and the impact on air quality.

The quantification of continental sources and sinks of CO₂ can be improved by regional inversion (the so-called top-down method). In this approach, the variability in atmospheric CO₂ concentrations are observed to better understand the causes of variability in the source-sink distribution by inverting the atmospheric transport. A number

CO₂ dispersion modelling over Paris

C. Lac et al.

Title Page

Abstract

Introduction

Conclusions

References

Tables

Figures

◀

▶

◀

▶

Back

Close

Full Screen / Esc

Printer-friendly Version

Interactive Discussion



**CO₂ dispersion
modelling over Paris**

C. Lac et al.

[Title Page](#)[Abstract](#)[Introduction](#)[Conclusions](#)[References](#)[Tables](#)[Figures](#)[◀](#)[▶](#)[◀](#)[▶](#)[Back](#)[Close](#)[Full Screen / Esc](#)[Printer-friendly Version](#)[Interactive Discussion](#)

of studies have used inverse modelling tools at global and regional scales (Enting, 1993; Rödenbeck et al., 2003; Gurney et al., 2002; Lauvaux et al., 2008, 2009) together with global networks of observations which also recently include tall tower observatories. But the scarcity of concentration measurements and errors in simulating atmospheric transport can introduce large uncertainties. Furthermore, the spread in fluxes induced by transport model differences was found to be almost as large as the uncertainties arising from the lack of adequate observations (Gurney et al., 2002). Using high resolution atmospheric models to retrieve CO₂ sources and sinks at the regional scale represents a major progress, as shown by the model intercomparison study over Europe led by Geels et al. (2007).

The major uncertainties in CO₂ modelling are related to model errors in horizontal wind (Lin and Gerbig, 2005) and vertical transport within the Atmospheric Boundary Layer (ABL) (Gerbig et al., 2008; Kretschmer et al., 2012). The boundary Layer Height (BLH) is a key variable in modelling atmospheric CO₂ since surface fluxes are mixed up to this height (“first order” approximation), causing the atmospheric CO₂ concentration to be underestimated when the BLH is overestimated, and vice versa, assuming a constant surface source. Geels et al. (2007) showed that in inversion CO₂ studies at low altitude sites, only the afternoon values of concentrations can be represented sufficiently well and are therefore more appropriate for constraining large-scale sources and sinks in combination with transport models, as the stable boundary conditions are highly difficult to represent by the meteorological models (Seibert et al., 2000). Therefore, inversion studies usually tend to impose less statistical weighting (larger uncertainty) or implement temporal data filtering (e.g. selection of afternoon data). Lauvaux et al. (2008) also found that improving the transport simulation for nocturnal CO₂ concentrations at tower sites would lead to large error reduction in CO₂ inversions. In this context, a correct representation of the ABL during the night and the morning is challenging.

Also during daytime, Sarrat et al. (2007b), in an intercomparison study of five mesoscale models, showed that BLHs between models revealed considerable

**CO₂ dispersion
modelling over Paris**

C. Lac et al.

[Title Page](#)[Abstract](#)[Introduction](#)[Conclusions](#)[References](#)[Tables](#)[Figures](#)[◀](#)[▶](#)[◀](#)[▶](#)[Back](#)[Close](#)[Full Screen / Esc](#)[Printer-friendly Version](#)[Interactive Discussion](#)

discrepancies. The BLH can also be affected by entrainment from overshooting thermals that is often underestimated in mesoscale meteorological models (McGrath-Spangler and Denning, 2010). De Arellano et al. (2004) have shown that the CO₂ concentration in the ABL is reduced much more effectively by the ventilation with entrained air than by CO₂ uptake by the vegetation, especially in the morning hours during the rapid growth of ABL.

Detailed validations of high-resolution forward models using networks of atmospheric measurements are therefore needed to assess how well the transport and variability of atmospheric tracers are represented. A number of studies using high-resolution models showed substantial improvements in simulating atmospheric CO₂ concentrations under various mesoscale flow conditions (Sarrat et al., 2007a; Ahmadov et al., 2009; Perez-Landa et al., 2007). In this context, urban areas are challenging to represent for CO₂ inversion studies: they add to the variability of the BLH, and Angevine et al. (2003) pointed out the important implications of urban-rural contrasts for air quality. But they also present the advantage of a Nocturnal Boundary Layer (NBL) that is mixed compared to the rural one. If the urban effects are well represented, this can limit the errors of the model generally associated to the stable boundary conditions. The performance of urban surface parameterisations are therefore crucial in simulating Urban Boundary Layer (UBL) (Lemonsu et al., 2006; Lee et al., 2008).

This work, as part of the CO₂-MEGAPARIS project, uses a high-resolution modelling approach with the Meso-NH model to investigate the variability of CO₂ concentration as well as BLH over Paris agglomeration. During the CO₂-MEGAPARIS campaign from 21–26 March 2011, anticyclonic weather conditions prevailed (clear sky, moderate temperatures and light winds). Pal et al. (2012) already investigated in detail the spatio-temporal variability of the observed BLH without including CO₂ measurements and they focussed mainly on the first four days of the campaign to assess the impact of Urban Heat Island (UHI) on the boundary layer circulations.

The main goals of our study are (1) to test the ability of high-resolution models to represent the spatial and temporal variability of BLH and CO₂ over urban and

sub-urban areas, (2) to infer the effect of urban-rural contrasts on the observed atmospheric CO₂ field and (3) to assess the possibility of using these modelling tools in future inversion studies. This paper begins by providing an outline of the modelling strategy and the CO₂-MEGAPARIS dataset, including a description of the specifics of the model setup and the experimental domain (Sects. 2 and 3). This is followed by a validation and discussion of the meteorological predictions against observational data (Sect. 4). The ability of the mesoscale modelling system to reproduce the variability of CO₂ concentration is then examined in urban, sub-urban and rural sites (Sect. 5). Impact studies of urban surface parameterisation and anthropogenic emissions are led to help analyzing CO₂ emissions and dilution. A summary and discussion on dominant uncertainties in inverse modelling of CO₂ fluxes follow in Sect. 6.

2 Modelling strategy with MESO-NH

The MESO-NH model (Lafore et al., 1998) is a non-hydrostatic meso-scale model developed by Météo-France and Laboratoire d'Aérodynamique for research purposes (see <http://mesonh.aero.obs-mip.fr/mesonh/>). The model has been widely used to investigate the CO₂ cycle (Sarrat et al., 2007a,b, 2009; Noilhan et al., 2011). In this study the model has been run at 2 km horizontal resolution over a domain of 500 km × 500 km covering Northern France, the southeast of England and most of Belgium, as shown in Fig. 1a. The vertical resolution is minimum (18 m) near the surface and 2 km at the top of the domain above 20 km, leading to 46 levels with 21 levels in the first 2 km. An overview of the model set up, dynamical parameters, and model physics used is given in Table 1. The atmospheric model assumes the CO₂ mixing ratio transported as a passive scalar. In the following, we will improperly call mixing ratio by concentration.

The MESO-NH model runs in-line with the land surface-atmosphere interaction model SURFEX (Masson et al., 2012), including four components representing ocean, inland waters, urban areas and vegetation, corresponding to the surface types in the land cover ECOCLIMAP II (Masson et al., 2003), which has a resolution of 1 km and

CO₂ dispersion modelling over Paris

C. Lac et al.

Title Page

Abstract

Introduction

Conclusions

References

Tables

Figures

◀

▶

◀

▶

Back

Close

Full Screen / Esc

Printer-friendly Version

Interactive Discussion



**CO₂ dispersion
modelling over Paris**

C. Lac et al.

Title Page

Abstract

Introduction

Conclusions

References

Tables

Figures

◀

▶

◀

▶

Back

Close

Full Screen / Esc

Printer-friendly Version

Interactive Discussion



includes 273 ecosystems. Most important components included in the surface model for this study are the urban and vegetation schemes, the Town Energy Balance (TEB) (Masson, 2000) and Interactions between Soil, Biosphere, and Atmosphere (ISBA-A-gs) (Calvet et al., 1998; Noilhan and Planton, 1989) respectively. The TEB model was previously validated and has shown to reproduce well surface fluxes in urban areas both in offline mode (Hamdi and Masson, 2008) and online with MESO-NH (Masson, 2006; Lemonsu et al., 2006; Hidalgo et al., 2008). ISBA-A-gs includes CO₂ assimilation by the vegetation and ecosystem respiration to compute on-line the surface energy and CO₂ fluxes. The latent heat flux as well as the carbon flux are computed through a stomatal conductance. ISBA-A-gs uses a tile approach, in which each grid cell is divided into a maximum of 12 patches of natural or vegetation types (bare soil, snow, rock, tree, coniferous, evergreen, C3 crops, C4 crops, irrigated crops, grassland and parks). Noilhan et al. (2011) have shown a significant improvement of the ABL representation by fully coupling CO₂ between surface and atmosphere using the tiling approach. The SURFEX scheme diagnoses the 2 m temperature and humidity, and 10 m wind with a specific algorithm (Masson and Seity, 2009), that implements a 1-D prognostic turbulence scheme on 6 vertical levels inserted between the surface and the lowest atmospheric model level (9 m here).

The anthropogenic CO₂ emissions are obtained from an inventory (10 km resolution) provided by University of Stuttgart (Dolman et al., 2006). Oceanic CO₂ fluxes are parameterised following Takahashi et al. (1997).

Each day of the campaign is simulated by a single, 24 h model run, initialised and coupled each 3 h with the analysis from the 2.5 km resolution operational model of AROME (Seity et al., 2010) for the meteorological fields. The first day's CO₂ field was initialised with the CO₂ background concentration measurement at Eiffel Tower (minimum value of the day), with a homogeneous vertical profile, horizontally consistent across the entire model domain, while the other days used the predicted CO₂ field from the end of the previous day as a starting concentration field. The boundary conditions CO₂ profiles during each day's simulations were also taken from the homogeneous

vertical profiles. Three simulations are performed using same model configuration, i.e. same domains, initialisation fields and physical parameterisations: (1) the first simulation (henceforth REF, as the reference) is performed with the whole surface schemes; (2) the second simulation (RUR hereafter) is conducted without the TEB urban scheme (the urban land-use covers are replaced by rock, treated by ISBA) in order to quantify the effect of the urban parameterisation; (3) the third simulation corresponds to REF for the surface schemes but without CO₂ anthropogenic emissions (hereafter NAN).

3 Brief presentation of the CO₂-MEGAPARIS March campaign

The CO₂-MEGAPARIS March experiment field served as a testbed for the project (see <http://co2-megaparis.lsce.ipsl.fr>): it started on 21 March and ended on 26 March 2011. The meteorological network (described in Pal et al., 2012) was constituted of 3 vertically-pointing aerosols lidars and a ceilometer observing quasi-continuous evolution of the BLH operating at the Jussieu (hereafter JUSS) campus in the center of Paris (Fig. 1b), at the SIRTAs observatory representative of a sub-urban site and located at about 20 km south of Paris, and at Trainou (hereafter TRN) located in the south of Paris at a distance of around 100 km, served as a rural background reference site (Fig. 1a). Additionally, radiosounding measurements with a frequency of twice-a-day (00:00 and 12:00 UT) were performed at the French operational station Trappes (hereafter TRAP) located in the western suburb of Paris (15 km west of SIRTAs). Also the French operational surface network includes 270 stations on the simulation domain to evaluate temperature and relative humidity at 2 m and wind fields at 10 m (Fig. 2). The CO₂ monitoring network includes ground CO₂ concentration measurements at Gif-sur-Yvette (GIF) located 30 km in the south-west of Paris and 8 km west of Orly-Airport, at Gonesse (GON) on the North-East of Paris, 3 km west of Paris-CDG airport, at Montge-en-Goelle (MON), a rural station located 10 km east of Paris-CDG airport and also at the rural site of TRN (only for 21 March). Additionally, CO₂ concentration measurements were carried on at the top of the Eiffel tower (310 m, EIF). The CO₂ monitoring stations

Title Page

Abstract

Introduction

Conclusions

References

Tables

Figures

◀

▶

◀

▶

Back

Close

Full Screen / Esc

Printer-friendly Version

Interactive Discussion



at GIF and TRN are part of the ICOS infrastructure (<http://www.icos-infrastructure.eu/>) while the EIF, GON and MON instrumentations were deployed in 2010 within the CO₂-MEGAPARIS project (<http://co2-megaparis.lsce.ipsl.fr>) and integrated into AIRPARIF network infrastructures. In each station, a ring-down cavity analyser from PICARRO model G1301 was deployed.

The meteorology during the first 4 days of the study period was characterised by anticyclonic conditions over North-West of Europe, maintaining a dry and sunny weather over most of France. On Paris area, it leads to weak north-easterly winds and temperatures progressively increasing and reaching a maximum of 21 °C on 24 March. On 25 March the winds became very weak due to the formation of a ridge between high pressure regions stretching from north-west of Ireland, through France and past the southern tip of Italy. This ridge began to break up on 26 March as a low pressure cell moves in from the Atlantic. On the Ile-de-France province, the wind rotated to the south-west and the sky became cloudy. This has resulted in two meteorological regimes during the study period, with the transition day between them on 25 March.

4 Meteorological results

The performance of the Meso-NH simulations is first evaluated against boundary layer observations. The meteorological measurements considered are: (1) The 2 m air temperature (T2M) and relative humidity (HU2M) and 10 m wind fields observed at numerous meteorological stations: 235 hourly stations for T2M and HU2M and 113 stations for wind fields are considered every day extending over the domain (Fig. 2). (2) T2M at urban (Paris-Montsouris), sub-urban (SIRTA) and rural (TRN) stations during the campaign. (3) The potential temperature vertical profile from the radiosounding (RS) at TRAP. (4) Surface heat fluxes measured at SIRTA. (5) The BLH measured by the lidar systems at the 3 stations (TRN, SIRTA, JUSS).

CO₂ dispersion modelling over Paris

C. Lac et al.

Title Page

Abstract

Introduction

Conclusions

References

Tables

Figures

◀

▶

◀

▶

Back

Close

Full Screen / Esc

Printer-friendly Version

Interactive Discussion



4.1 Reference simulation evaluation: Urban Heat Island (UHI)

Evaluating meteorological simulations against T2M, HU2M and 10 m wind fields is often performed in operational weather prediction centers. The scores are generally difficult to improve and are very informative of the quality of the surface and boundary layer simulation. A synthesis of the mean biases and root mean square errors (rmse) is given in Fig. 3 for the REF simulation. In order to evaluate separately TEB and ISBA schemes, the scores are separated between urban and sub-urban stations in one side (corresponding to a town fraction greater than 0.1, leading to 35 stations over 235 for T2M) and rural stations (town fraction less than 0.1) on the other side. Statistical scores show a good behavior of the REF simulation, with a bias less than 1.8°C for T2M, 6% for HU2M, 0.8 ms^{-1} and 20° for the wind speed and direction, respectively. The deviation from the measurements (rmse) is a bit higher. There is an indication of diurnal trend in the statistics of bias: for the set of stations (red curve), the predicted atmospheric regime is slightly too cold and too wet during the day, and in very good agreement during the night, as illustrated on Fig. 2 for 23 March at 04:00 and 11:00 UT. For urban stations, a small positive bias appears on temperature and humidity during the whole day except the morning, meaning that the TEB scheme tends to overpredict the UHI, up to 0.5°C during the night. A possible explanation is that the surrounding of urban stations is often characterised by a high portion of urban vegetation that is underestimated at 2 km horizontal resolution and by the 1 km ECOCLIMAP data. Also the parks and vegetated spaces embedded in an urban/suburban surrounding are not considered by the TEB scheme; this will be a further improvement of the urban parameterisation (Lemonsu et al., 2012). On the contrary, the excessive surface cooling and moistening during the day is mainly attributed to the ISBA scheme. Deviations from the measurements (rmse) are equivalent for urban and rural stations. The wind speed is slightly overestimated during the night, especially on the rural stations, and underestimated at the end of the morning, particularly for urban stations. The error on the wind direction is small and fluctuating, with a high deviation, due to the fact that the wind

Title Page

Abstract

Introduction

Conclusions

References

Tables

Figures

◀

▶

◀

▶

Back

Close

Full Screen / Esc

Printer-friendly Version

Interactive Discussion



speed is very weak during the period, making the prediction difficult. Scores are very similar for all the days of the period (not shown).

Figure 4 shows the time series of the near surface air temperature measured and predicted at urban (Paris-Montsouris), sub-urban (SIRTA) and rural (TRN) stations during the campaign. The upper panel exemplifies the classical diurnal cycle of observed temperature, with here an increasing trend over all sites until 25 March and a change during 26 March. The daily maximum temperature observed at Paris increases from 15°C on 21 March to 21°C on 25 and decreases to 17°C on 26, while the minimum temperature increases from 5°C on 21 March to 14°C on 25 March, and remains constant on 26 March. The higher increase of minimal temperatures than maximal temperatures is a signature of the thermal accumulation effect in the urban area (Pal et al., 2012). The difference of temperature between the urban site on one side, and the sub-urban and rural sites on the other side are representative of the UHI, which is stronger at night than during day. It is noteworthy that the contrast between the three sites is negligible during sunrise, and more significantly on 25 March until the maximum of the ABL convective mixing, due to the absence of wind all over the domain inducing a generalized strong heating. Also, the dry previous days have reduced the soil moisture at the rural site and evapotranspiration by the vegetation becomes therefore small.

The middle panel represents the predicted temperature on the same sites for the REF simulation. The discontinuity sometimes present at 00:00 UT for the different days corresponds to the analysis from AROME model that initialises the new Meso-NH daily simulation. It is noteworthy that only the measurements at Paris-Montsouris are included in the data assimilation in AROME, inducing the same T2M between observation (Fig. 4a) and initial conditions of the run (Fig. 4b) at midnight, on the contrary to the occasional measurements at SIRTA and TRN sites, not taken into account in the operational analysis. The REF simulation reproduces well the increasing trend of the temperature and the urban-rural contrasts, with only a systematic overestimation of the maximum temperature at the urban site of 2°C. Indeed, Montsouris station is a good example of an urban station embedded in a park, whose effects on surface fluxes are

**CO₂ dispersion
modelling over Paris**

C. Lac et al.

[Title Page](#)[Abstract](#)[Introduction](#)[Conclusions](#)[References](#)[Tables](#)[Figures](#)[◀](#)[▶](#)[◀](#)[▶](#)[Back](#)[Close](#)[Full Screen / Esc](#)[Printer-friendly Version](#)[Interactive Discussion](#)

not considered, as mentioned before. However, the UHI intensity is well represented during the night.

These results illustrates the fact that the REF simulations closely match the observations and can capture the urban-rural contrasts fairly well.

4.2 Boundary layer height (BLH)

Figure 5 shows vertical profiles of potential temperature above TRAP at 00:00 and 12:00 UT for the REF simulation, compared to the daily soundings. The sonde drifting has been neglected for the simulation comparison as the wind in the ABL is weak during the period. In agreement with the previous scores, the surface temperature at this sub-urban site tends to be slightly underestimated during the day, and overestimated during the night. At midday, the convective mixing is fairly reproduced except on 21 March, where the BLH is slightly underpredicted. At midnight, the nocturnal positive potential temperature gradient is generally well represented with however a small underestimation on 25 and 26 March inherent to the small positive bias on surface temperature. Steeneveld et al. (2008) have underlined the frequent underestimation of the stratification of nighttime surface inversions in mesoscale models, pointed out the difficulty to parameterise stable boundary conditions. However, the model tends to capture well the potential temperature profiles. To evaluate more accurately the BLH predictions, BLH are extracted from lidar and Ceilometer measurements, following the method discussed in Pal et al. (2010), and compared to the model diagnostics. The diagnosis of the BLH in the model is based on the TKE profile (the first level from the ground with a TKE less than 10% of the near surface value determines the BLH) (Seibert et al., 2000). For 25 and 26 the lidar was not useful at SIRTAsite for technical problem and therefore only ceilometer was used, reducing the quality of BLH estimation. Also the lidar system was not able to result the BLH over the rural site during nighttime since full overlap of the lidar system is reached at a height of around 150 m AGL.

CO₂ dispersion modelling over Paris

C. Lac et al.

Title Page

Abstract

Introduction

Conclusions

References

Tables

Figures

◀

▶

◀

▶

Back

Close

Full Screen / Esc

Printer-friendly Version

Interactive Discussion



**CO₂ dispersion
modelling over Paris**

C. Lac et al.

[Title Page](#)[Abstract](#)[Introduction](#)[Conclusions](#)[References](#)[Tables](#)[Figures](#)[I◀](#)[▶I](#)[◀](#)[▶](#)[Back](#)[Close](#)[Full Screen / Esc](#)[Printer-friendly Version](#)[Interactive Discussion](#)

Figure 6 shows time series of the BLH for the urban (JUSS), sub-urban (SIRTA) and rural (TRN) sites, with comparison between observations and simulations. During daytime, measurements show significant contrasts between the 3 sites with the deepest mixing for JUSS, than SIRTA and TRN. However, the first four days, these differences are limited (maximum of 200 m between JUSS and TRN), and the maximum BLH remains quite constant for all the days even if the near ground temperature increases (Fig. 4a). The highest contrast between urban and rural sites during daytime occurs on 25 March with a difference of 600 m at 14:00 UT, while near ground surface temperatures differ only from 1 °C between rural and urban sites. This is probably due to high values of daytime evapotranspiration at TRN. 26 March is characterised by a weaker BLH than the previous day and some fluctuations at SIRTA and TRN due to the change in the prevailing meteorological regime. During nighttime, where the BLH is determinant for the pollutant concentrations, measurements show maximum BLH differences between JUSS and SIRTA sites of the order of 100 m.

The REF simulation captures reasonably well the BLH for all the sites during daytime, with negative biases between 85 m and 122 m (Table 2). In the morning, the onset time of the ABL mixing and the growth rate of the BLH are particularly well reproduced. Maxima of BLH are also well captured, except a slight underprediction the first two days for the 3 sites. The increase of daytime BLH on 25 March is correct on the urban and sub-urban sites, while it is overestimated on the rural site, as well as on 26 March for the 3 sites. During nighttime, the REF simulation represents fairly well the shallow mixing depth over urban and sub-urban sites, with only small negative biases of 47 m and 34 m respectively (Table 2). Underestimations occur at JUSS on 25–26 March, and at SIRTA on 21, 24–25 and 25–26 March (but BLH measurements at SIRTA are not so reliable on 25–26 March). The small underprediction of the nocturnal BLH for these 3 nights at SIRTA site is also visible on the sensible heat flux that is slightly underestimated (Fig. 6d).

4.3 Importance of the urban scheme

The evaluation of the RUR simulations is compared to the REF ones for T2M, HU2M and 10 m wind at the urban stations (Fig. 7). The absence of urban scheme logically translates the bias curve to weaker temperatures (higher humidities) similarly for each hour, increasing the negative bias of T2M (positive bias of HU2M) during the day and reducing the positive bias of T2M (negative bias of HU2M) during the night. It also increases slightly the negative biases of the wind speed during the day, meaning that the absence of urban-rural contrasts reduces the wind. The discrepancies on the wind direction are also increased without the urban scheme. The absence of urban scheme has therefore a negative impact as it removes the urban-rural contrasts, and the associated circulations (Hidalgo et al., 2008). On Fig. 4c, the RUR simulation underestimates systematically the urban temperature (the corrections by the analysis at 00:00 UT are important) and removes the UHI: the small differences between the three sites are only linked to the orography effect of the Paris bassin and to the cooling associated to the evapotranspiration for the rural site compared to the rock replacing the urban area in the RUR simulation.

The comparison between REF and RUR simulations on the BLH (Fig. 6) shows that both predict similar daytime BLH on urban and sub-urban sites except for 25 March, as it is largely underpredicted over JUSS and SIRTA without TEB. Therefore the biases of BLH for the RUR simulation during daytime are twice the ones of the REF simulation on JUSS and SIRTA, with a rmse also increased (Table 2). Systematically, the RUR simulation underpredicts the nighttime BLH on the urban and sub-urban sites (doubled biases), showing the effectiveness of the TEB scheme in representing the storage of heat in urban materials during the night. The impact at the sub-urban site is smaller but not negligible all the nights.

CO₂ dispersion modelling over Paris

C. Lac et al.

Title Page

Abstract

Introduction

Conclusions

References

Tables

Figures

◀

▶

◀

▶

Back

Close

Full Screen / Esc

Printer-friendly Version

Interactive Discussion



5 CO₂ distribution in regional scale

CO₂ concentration predictions are investigated herein using time series of predictions from REF, RUR and also NAN simulations against observations, for the Eiffel Tower (hereafter EIF), Gonesse (GON), Montge-en-Goelle (MON), Gif-sur-Yvette (GIF) and Trainou (TRN). The NAN simulation allows to distinguish the sites quasi-fully influenced by anthropogenic emissions (EIF) and those strongly influenced by anthropogenic emissions (GON and GIF), to the site both exposed to anthropogenic and biogenic emissions (MON) and finally to the rural site quasi fully driven by assimilation and plant transpiration (TRN). It is worth noting that peak values of anthropogenic emissions over Paris and its airports occur during rush hours, between 08:00 and 10:00 UT, and 17:00 and 19:00 UT (not shown).

5.1 Evaluation at the urban site: Eiffel Tower

As JUSS is close to EIF and its lidar measurements fairly represent the BLH over Paris, instrumental extractions of BLH at this location have been compared to BLH predictions at EIF (Fig. 8a) to help analyzing CO₂ predictions and observations at EIF (Fig. 8b).

The observed spikes of CO₂ maxima occur generally between 08:00 and 10:00 UT, exactly at the time (vertical dashed line) at which the BLH growth reaches the measurement height on the Eiffel Tower (310 m as shown in Fig. 8a). These spikes have a very short duration as the ABL grows quickly, favoring the rapid mixing of pollutant on a deeper layer and consequently the rapid CO₂ concentration decrease. A prediction error appears during the night of 22–23 March and the early morning, with higher observed concentrations on a period of several hours, probably due to a deeper NBL reaching the height measurement (observed BLH at JUSS were not available this night).

The modelled concentrations can be seen to agree very well with observations in terms of timing and temporal evolution: predicted and observed maxima occur at the same time, meaning that the predicted BLH reaches 310 m at the right time. The

CO₂ dispersion modelling over Paris

C. Lac et al.

Title Page

Abstract

Introduction

Conclusions

References

Tables

Figures

◀

▶

◀

▶

Back

Close

Full Screen / Esc

Printer-friendly Version

Interactive Discussion



**CO₂ dispersion
modelling over Paris**

C. Lac et al.

[Title Page](#)[Abstract](#)[Introduction](#)[Conclusions](#)[References](#)[Tables](#)[Figures](#)[I◀](#)[▶I](#)[◀](#)[▶](#)[Back](#)[Close](#)[Full Screen / Esc](#)[Printer-friendly Version](#)[Interactive Discussion](#)

predicted CO₂ peak are also very brief, in agreement with measurements. The longer period of higher concentrations during the night of 22–23 March is slightly underestimated due to an underprediction of the BLH, whereas the REF simulation tends to produce higher BLH than for the other nights, reaching punctually the EIF measurement height. One discrepancy occurs on 25 March at 02:00 UT, as the model predicts a peak of 450 ppm that does not occur in reality, associated to a reservoir of pollutant in the simulated residual layer. In terms of intensity, there are small biases on CO₂ concentrations, that could be linked to the misrepresentation of the anthropogenic emissions. For instance, the strongest peak measured at EIF during the campaign occurs on 25 March at 11:00 UT as a consequence of the negligible wind during all the night and the early morning (Fig. 9). Anthropogenic CO₂ accumulates over Paris intra-muros in the Seine valley in the shallow early morning ABL (Fig. 9c at 08:00 UT) and this reservoir reaches 300 m height with the ABL growing at 11:00 UT (Fig. 9d). The model underpredicts the maximum over Eiffel Tower but reproduces CO₂ concentration magnitudes at 300 m comparable to the measurements magnitude over the eastern part of Paris town (Fig. 9f with measurement in coloured square). The predicted plume concentration are directly linked to the CO₂ emissions that are higher on the eastern part of Paris. It is therefore likely that the underestimation at EIF is mainly due to the too coarse anthropogenic emissions, as the correct concentrations have been produced on another part of Paris. Moreover, the simulated ground level concentrations closely match the lower observed concentration values at the sub-urban sites (Fig. 9e). So the general anthropogenic pollutant accumulation over Paris city on 25 March is correctly reproduced: its representation at local scale could be improved with finer emission inventories.

The RUR does not significantly modify CO₂ predictions at EIF because the absence of TEB does not impact significantly the growing phase of the ABL whereas it would modify concentrations at ground level.

5.2 Evaluation at the sub-urban and rural sites

CO₂ concentration observations and predictions at the sub-urban and rural sites are presented in Fig. 10. GIF is located in the sub-urban site close to the SIRTA and so that we can gain a good understanding on the influence of BLH on CO₂ concentrations by comparing Figs. 6b and 10c. On the contrary to EIF measuring altitude concentrations, the surface sub-urban sites always exhibits maxima during the night when the BLH is fully contracted. Maxima reach 450 ppm the first four nights for the sub-urban site, and more than 500 ppm the following nights. Both GON and GIF measurements exhibit a strong temporal variability of CO₂ concentration, up to 100 ppm nocturnal amplitude. Comparatively, the maximum amplitude at MON site reaches 50 ppm between night and day (Fig. 10b), while it is systematically of 20 ppm at TRN (Fig. 10d).

At GIF site (Fig. 10c), the REF simulation reproduces correctly the timing of the diurnal cycle of CO₂ concentration. The minimal CO₂ concentration are well captured by the model. Indeed, the small differences on the diurnal maximum BLH between observation and REF prediction on one side, and between REF and RUR simulations on the other side, do not appear, as the convective mixing is high.

During the night, the timing of maxima of CO₂ concentration at the beginning and at the end of each night is well reproduced. The discrepancies concern the intensity of nocturnal peaks, sometimes overpredicted. When the predicted BLHs are in agreement with observations (e.g. nights of 21–22 and 22–23), overprediction of CO₂ concentration is of the order of 30 ppm, meaning that errors on the emissions at rush hours are probably responsible. When the BLH is underpredicted (nights of 21, 23–24 and 24–25), the discrepancy exceeds 60 ppm. The highest one (100 ppm) occurs the night of the 24–25 at midnight, corresponding to the underprediction of the nocturnal BLH of approximately 100 m at SIRTA (Fig. 6b). Consequently, the RUR simulations, adding significant vertical transport errors associated to the BLH underprediction, exhibit additional significant errors compared to the REF simulation, underlying the necessity of the urban scheme.

Title Page

Abstract

Introduction

Conclusions

References

Tables

Figures

◀

▶

◀

▶

Back

Close

Full Screen / Esc

Printer-friendly Version

Interactive Discussion



**CO₂ dispersion
modelling over Paris**

C. Lac et al.

Title Page

Abstract

Introduction

Conclusions

References

Tables

Figures

◀

▶

◀

▶

Back

Close

Full Screen / Esc

Printer-friendly Version

Interactive Discussion



At GON, predicted CO₂ concentrations reproduce fairly well the observed diurnal cycle, in terms of timing and maxima and minima magnitudes (Fig. 10a). The only discrepancies are small underestimations of the CO₂ concentration peaks during the nights of 21–22, 22–23 and 25–26. Even if BLH are not measured at this site, these small errors are not attributed to the vertical transport as REF and RUR predicted concentrations are very close, but to the wind direction: the model predicts north-east or north instead of east-north-east wind direction for very weak winds, and thus minimizes the impact of CDG airport plume on GON. The only small overestimation of CO₂ concentration occurs the morning of 25 March, due to a delay in the predicted development of the convective ABL associated to an underestimation of the near ground temperature on the North-East of Paris (Fig. 9a, b). To summarize, the small discrepancies of CO₂ concentration at the sub-urban sites GIF and GON illustrate the main well-known sources of uncertainties of the meteorological model: the vertical transport for GIF, as located in the plume of Paris during the March campaign and the horizontal transport for GON, in the plume of CDG airport.

The CO₂ concentrations at MON, classified as a rural site, are nevertheless influenced by anthropogenic emissions from Paris and CDG airport, as the difference between REF and NAN simulations is no negligible (Fig. 10b). The period exhibits two regimes, with a quite regular diurnal cycle the first 4 days and a maximum of 430 ppm, and a strong variability the 2 last days with 2 stronger peaks due to the weak winds with variable directions including mainly westerly winds. The model reproduces fairly well these two regimes, with only a small underestimation of 10 ppm on 23 and 24 March and on 26 March in the morning.

While almost no observations are available for the rural site of TRN during this period, the measurements at the beginning of the period allow to check the predicted concentration. The CO₂ diurnal cycle is almost identical each day of the period, with a nocturnal maximum due to the ecosystem respiration (Fig. 10d), and a CO₂ concentration decrease in the ABL when the BLH increases, due to CO₂ vertical mixing but also to photosynthesis activity which depletes the boundary layer CO₂ concentration.

The three simulations REF, RUR and NAN are almost superimposed, meaning that the vegetation fully drives the diurnal cycle of carbon.

5.3 CO₂ horizontal heterogeneity in the well-mixed ABL

Figure 10 shows that the model reproduces well the midday lower concentrations at the different sites. Even if strong convective mixing in the ABL during daytime induce lower concentration values, urban-rural contrasts can lead to significant horizontal gradients and also moderate variability from one day to another. For instance, on 25 March at 15:00 UT, the weak winds favor the higher BLH over the city (Fig. 11c). Horizontal CO₂ gradients reach up to 25 ppm between GIF and GON (Fig. 11d). This is correctly reproduced by the model. The predicted concentration over MON is overpredicted by 10 ppm, but the station is located on the border of the predicted plume and the accuracy of the anthropogenic emissions is not sufficient to get so fine plumes resolution. The situation differs from the previous days when the northeasterly stronger winds dilute the urban heat fluxes, transporting away the urban dome and homogenizing the BLH (Fig. 11a). The CO₂ plume is advecting downwind above the south-west of Paris, inducing the maximum concentration values of the measurement stations at GIF site (Fig. 11b). The discrepancies between measurements and predictions are very small, between 1 and 2 ppm over the 3 stations.

6 Conclusions

In order to better understand the effects that mesoscale transport has on atmospheric CO₂ distributions in urban and sub-urban areas, the mesoscale atmospheric model Meso-NH coupled with the Town-Energy balance (TEB) urban canopy scheme and with the Interactions between Soil, Biosphere and Atmosphere CO₂-reactive (ISBA-A-gs) surface scheme has run for the period from 21 March to 26 March in 2011 covering the campaign of CO₂-MEGAPARIS project. The validation of forward modelling of CO₂

CO₂ dispersion modelling over Paris

C. Lac et al.

Title Page

Abstract

Introduction

Conclusions

References

Tables

Figures

◀

▶

◀

▶

Back

Close

Full Screen / Esc

Printer-friendly Version

Interactive Discussion



transport is essential to validate the system and also to show its potential in the context of inverse modelling when using high-frequency CO₂ concentration data. For rural stations, it is well-known that only afternoon values of CO₂ concentration are well appropriate for estimating carbon sources/sinks on land, and preferentially for data sampled several hundred meters above ground, as they can be represented substantially more robustly in atmospheric models (Geels et al., 2007). In this context, the objective of our study was to assess the capability of the modelling system to be used on urban and sub-urban area in inverse studies.

During daytime, the model captures well the onset time of the BLH thickening in the morning, as well as the growth rates at all the different sites. Indeed, the timing of CO₂ concentration spikes at Eiffel tower, occurring when the BLH reaches the measurement height, is remarkably well reproduced corresponding to the growing phase of the ABL. Also, at the ground stations, minimum predicted and measured concentrations are in agreement, with significative horizontal gradients linked to urban-rural contrasts. This suggests to apply inversion during daytime on urban and sub-urban area not only the afternoon but including the morning, and not only for tower sites but also for ground stations.

During nighttime in urban area, the difficulty for the models to reproduce the vertical transport correctly is not so strong as for rural area due to the NBL mixing, avoiding the stable boundary layer conditions. However, observed nocturnal CO₂ concentrations show a high spatio-temporal variability on the sub-urban area with strong maxima at rush hours (at the beginning and at the end of the night) in the contracted ABL, that is challenging to simulate. Meso-NH succeeds to reproduce the timing of the nocturnal CO₂ concentration at urban and sub-urban sites. The small discrepancies are mainly linked to weak errors on the vertical transport for the ground stations located in the Paris plume (e.g. GIF), or on the horizontal transport for ground stations in the plume of an airport (e.g. GON), and also on the too coarse resolution of the anthropogenic inventories. The performance of the urban parameterisation scheme TEB is crucial

**CO₂ dispersion
modelling over Paris**

C. Lac et al.

[Title Page](#)[Abstract](#)[Introduction](#)[Conclusions](#)[References](#)[Tables](#)[Figures](#)[I◀](#)[▶I](#)[◀](#)[▶](#)[Back](#)[Close](#)[Full Screen / Esc](#)[Printer-friendly Version](#)[Interactive Discussion](#)

to reproduce the UHI, the urban-rural contrasts and the nocturnal BLH on urban and sub-urban sites, and consequently the concentration maxima.

The good representation of CO₂ concentration on urban and sub-urban sites during nighttime emphasizes the use of the modelling system in inverse framework with nocturnal surface and tower station records. The study also demonstrates the potential of the CO₂-MEGAPARIS stations to be used for inverse methods, as the stations are devoted to monitor long term measurements of CO₂ and offer an adequate and comprehensive database to quantify surface fluxes. The next step of the study is now to apply one year of Meso-NH forward modelling in the same configuration with the CO₂-MEGAPARIS measurement network for inverse methods.

Acknowledgements. This work has been partially supported by the CO₂-MEGAPARIS project funded by the Agence Nationale de Recherche. The authors wish to thank all those who worked to collect the data in the field, especially M. Schmidt and M. Lopez who provided measurements at TRN. Also thanks to C. Treguer and M. Kebe for their contribution to the scores computation. We would like to thank two anonymous reviewers for their helpful comments.



The publication of this article is financed by CNRS-INSU.

References

Ahmadov, R., Gerbig, C., Kretschmer, R., Körner, S., Rödenbeck, C., Bousquet, P., and Ramonet, M.: Comparing high resolution WRF-VPRM simulations and two global CO₂ transport models with coastal tower measurements of CO₂, Biogeosciences, 6, 807–817, doi:10.5194/bg-6-807-2009, 2009. 28159

28175

ACPD

12, 28155–28193, 2012

CO₂ dispersion modelling over Paris

C. Lac et al.

Title Page

Abstract

Introduction

Conclusions

References

Tables

Figures

◀

▶

◀

▶

Back

Close

Full Screen / Esc

Printer-friendly Version

Interactive Discussion



**CO₂ dispersion
modelling over Paris**

C. Lac et al.

[Title Page](#)[Abstract](#)[Introduction](#)[Conclusions](#)[References](#)[Tables](#)[Figures](#)[◀](#)[▶](#)[◀](#)[▶](#)[Back](#)[Close](#)[Full Screen / Esc](#)[Printer-friendly Version](#)[Interactive Discussion](#)

Angevine, W. M., White, A., Senff, C. J., Trainer, M., Banta, R. M., and Ayoub, M. A.: Urban-rural contrasts in mixing height and cloudiness over Nashville in 1999, *J. Geophys. Res.*, 108, 4092–4099, 2003. 28159

Bougeault, P. and Lacarrere, P.: Parameterization of orography-induced turbulence in a meso-beta scale model, *Mon. Weather Rev.*, 117, 1870–1888, 1989. 28181

Calvet, J.-C., Noilhan, J., Roujean, J.-L., Bessemoulin, P., Cabelguenne, M., Oliosio, A., and Wigneron, J.-P.: An interactive vegetation SVAT model tested against data from six contrasting sites, *Agric. Forest Meteorol.*, 92, 73–95, doi:10.1016/S0168-1923(98)00091-4, 1998. 28161

Cuxart, J., Bougeault, P., and Redelsperger, J.-L.: a multiscale turbulence scheme apt for LES and mesoscale modelling, *Q. J. Roy. Meteor. Soc.*, 126, 1–30, 2000. 28181

De Arellano, J. V.-G., Gioli, B., Miglietta, F., Jonker, H. J. J., Baltink, H. K., Hutjes, R. W. A., and Holtslag, A. A. M.: Entrainment process of carbon dioxide in the atmospheric boundary layer, *J. Geophys. Res.*, 109, D18110, doi:10.1029/2004JD004725, 2004. 28159

Dolman, A., Noilhan, J., Durand, P., Sarrat, C., Brut, A., Butet, A., Jarosz, N., Brunet, Y., Loustau, D., Lamaud, E., Tolk, L., Ronda, R., Miglietta, F., Gioli, B., Magliulo, E., Esposito, M., Gerbig, C., Korner, S., Galdemard, P., Ramonet, M., Ciais, P., Neininger, B., Hutjes, R., Elbers, J., Warnecke, T., Landa, G., Sanz, M., Scholz, Y., and Facon, G.: CERES, the CarboEurope Regional Experiment Strategy in Les Landes, south-west France, May–June 2005, *B. Am. Meteorol. Soc.*, 87, 1367–1379, 2006. 28157, 28161

Enting, I. G.: Inverse problems in atmospheric constituent studies: III Estimating errors in surface sources, *Inverse Probl.*, 9, 649–665, 1993. 28158

Forster, P., Ramaswamy, V., Artaxo, P., Bernsten, T., Betts, R., Fahey, D. W., Haywood, J., Lean, J., Lowe, D., Myhre, G., Ngang, J., Prinn, R., Raga, G., Schulz, M., and Dorland, R. V.: Changes in atmospheric constituents and in radiative forcing, in: *Climate Change 2007: The Physical Science Basis. Contribution of Working Group I to the Fourth Assessment Report of the Intergovernmental Panel on Climate Change*, Cambridge University Press, Cambridge, United Kingdom and New York, NY, USA, 2007. 28157

Geels, C., Gloor, M., Ciais, P., Bousquet, P., Peylin, P., Vermeulen, A. T., Dargaville, R., Aalto, T., Brandt, J., Christensen, J. H., Frohn, L. M., Haszpra, L., Karstens, U., Rödenbeck, C., Ramonet, M., Carboni, G., and Santaguida, R.: Comparing atmospheric transport models for future regional inversions over Europe – Part 1: mapping the atmospheric CO₂ signals, *Atmos. Chem. Phys.*, 7, 3461–3479, doi:10.5194/acp-7-3461-2007, 2007. 28158, 28174

**CO₂ dispersion
modelling over Paris**

C. Lac et al.

Title Page

Abstract

Introduction

Conclusions

References

Tables

Figures

◀

▶

◀

▶

Back

Close

Full Screen / Esc

Printer-friendly Version

Interactive Discussion



Gerbig, C., Körner, S., and Lin, J. C.: Vertical mixing in atmospheric tracer transport models: error characterization and propagation, *Atmos. Chem. Phys.*, 8, 591–602, doi:10.5194/acp-8-591-2008, 2008. 28158

5 Gurney, K. R., Law, R. M., Denning, A. S., Rayner, P. J., Baker, D., Bousquet, P., Bruhwiler, L., Chen, Y. H., Ciais, P., Fan, S., Fung, I. Y., Gloor, M., Heimann, M., Higuchi, K., John, J., Maki, T., Maksyutov, S., Masarie, K., Peylin, P., Prather, M., Pak, B. C., Randerson, J., Sarmiento, J., Taguchi, S., Takahashi, T., and Yuen, C. W.: Towards robust regional estimates of CO₂ Sources and Sinks Using Atmospheric Transport Models, *Nature*, 415, 626–630, 2002. 28158

10 Hamdi, R. and Masson, V.: Inclusion of a drag approach in the town energy balance (TEB) scheme: offline 1-D validation in a street canyon, *J. Appl. Meteorol. Clim.*, 47, 2627–2644, 2008. 28161

Hidalgo, J., Masson, V., and Pigeon, G.: Urban-breeze circulation during the CAPITOUL experiment: numerical simulations, *Meteorol. Atmos. Phys.*, 102, 243–262, 2008. 28161, 28168

15 Kretschmer, R., Gerbig, C., Karstens, U., and Koch, F.-T.: Error characterization of CO₂ vertical mixing in the atmospheric transport model WRF-VPRM, *Atmos. Chem. Phys.*, 12, 2441–2458, doi:10.5194/acp-12-2441-2012, 2012. 28158

Lafore, J.-P., Stein, J., Asencio, N., Bougeault, P., Ducrocq, V., Duron, J., Fisher, C., Hereil, P., Mascart, P., Masson, V., Pinty, J.-P., Redelsperger, J.-L., Richard, E., and Guerau de Arelano, J. V.: The Meso-NH Atmospheric simulation system. Part I: Adiabatic formulation and control simulations, *Ann. Geophys-Germany*, 16, 90–109, 1998. 28160

20 Lauvaux, T., Uliasz, M., Sarrat, C., Chevallier, F., Bousquet, P., Lac, C., Davis, K. J., Ciais, P., Denning, A. S., and Rayner, P. J.: Mesoscale inversion: first results from the CERES campaign with synthetic data, *Atmos. Chem. Phys.*, 8, 3459–3471, doi:10.5194/acp-8-3459-2008, 2008. 28158

25 Lauvaux, T., Pannekoucke, O., Sarrat, C., Chevallier, F., Ciais, P., Noilhan, J., and Rayner, P. J.: Structure of the transport uncertainty in mesoscale inversions of CO₂ sources and sinks using ensemble model simulations, *Biogeosciences*, 6, 1089–1102, doi:10.5194/bg-6-1089-2009, 2009. 28158

30 Lee, S.-H., Kim, S.-W., Angevine, W. M., Bianco, L., McKeen, S. A., Senff, C. J., Trainer, M., Tucker, S. C., and Zamora, R. J.: Evaluation of urban surface parameterizations in the WRF model using measurements during the Texas Air Quality Study 2006 field campaign, *Atmos. Chem. Phys.*, 11, 2127–2143, doi:10.5194/acp-11-2127-2011, 2011. 28159

**CO₂ dispersion
modelling over Paris**

C. Lac et al.

[Title Page](#)[Abstract](#)[Introduction](#)[Conclusions](#)[References](#)[Tables](#)[Figures](#)[◀](#)[▶](#)[◀](#)[▶](#)[Back](#)[Close](#)[Full Screen / Esc](#)[Printer-friendly Version](#)[Interactive Discussion](#)

- Lemonsu, A., Pigeon, G., Masson, V., and Moppert, C.: Sea-town interactions over Marseille: 3D urban boundary layer and thermodynamic fields near the surface, *Theor. Appl. Climatol.*, 84, 171–178, 2006. 28159, 28161
- Lemonsu, A., Masson, V., Shashua-Bar, L., Erell, E., and Pearlmutter, D.: Inclusion of vegetation in the Town Energy Balance model for modeling urban green areas, *Geosci. Model Dev. Discuss.*, 5, 1295–1340, doi:10.5194/gmdd-5-1295-2012, 2012. 28164
- Lin, J. C. and Gerbig, C.: Accounting for the effect of transport errors on tracer inversions, *Geophys. Res. Lett.*, 32, L01802, doi:10.1029/2004GL021127, 2005. 28158
- Masson, V.: A physically-based scheme for the urban energy budget in atmospheric models, *Bound.-Lay. Meteorol.*, 1994, 357–397, 2000. 28161
- Masson, V.: Urban surface modeling and the meso-scale impact of cities, *Theor. Appl. Climatol.*, 84, 35–45, 2006. 28161
- Masson, V. and Seity, Y.: Including atmospheric layers in vegetation and urban offline surface schemes, *J. Appl. Meteorol. Clim.*, 48, 1377–1397, 2009. 28161
- Masson, V., Champeaux, J.-L., Chauvin, C., Meriguet, C., and Lacaze, R.: A global database of land surface parameters at 1 km resolution for use in meteorological and climate models, *J. Climate*, 16, 1261–1282, 2003. 28160
- Masson, V., Moigne, P. L., Martin, E., Faroux, S., Alias, A., Alkama, R., Belamari, S., Barbu, A., Boone, A., Bouyssel, F., Brousseau, P., Brun, E., Calvet, J.-C., Carrer, D., Decharme, B., Delire, C., Donier, S., Essaouini, K., Gibelin, A.-L., Giordani, H., Habets, F., Jidane, M., Kerdraon, G., Kourzeneva, E., Lafaysse, M., Lafont, S., Brossier, C. L., Lemonsu, A., Mahfouf, J.-F., Marguinaud, P., Mokhtari, M., Morin, S., Pigeon, G., Salgado, R., Seity, Y., Taillefer, F., Tanguy, G., Tulet, P., Vincendon, B., Vionnet, V., and Voldoire, A.: The SURFEXv7.2 land and ocean surface platform for coupled or offline simulation of Earth surface variables and fluxes, *Geosci. Model Dev. Discuss.*, submitted, 2012. 28160
- McGrath-Spangler, E. and Denning, A.: Impact of entrainment from overshooting thermals on land-atmosphere interactions during summer 1999, *Tellus*, 62, 441–454, doi:10.1111/j.1600-0889.2010.00482.x, 2010. 28159
- Noilhan, J. and Planton, S.: A simple parameterization of land surface processes for meteorological models, *Mon. Weather Rev.*, 117, 536–549, 1989. 28161
- Noilhan, J., Donier, S., Lacarrère, P., Sarrat, C., and LeMoigne, P.: Regional scale evaluation of a land surface scheme from atmospheric boundary layer observations, *J. Geophys. Res.*, 116, D01104, doi:10.1029/2010JD014671, 2011. 28160, 28161

**CO₂ dispersion
modelling over Paris**

C. Lac et al.

Title Page

Abstract

Introduction

Conclusions

References

Tables

Figures

◀

▶

◀

▶

Back

Close

Full Screen / Esc

Printer-friendly Version

Interactive Discussion



Pal, S., Behrendt, A., and Wulfmeyer, V.: Elastic-backscatter-lidar-based characterization of the convective boundary layer and investigation of related statistics, *Ann. Geophys.*, 28, 825–847, doi:10.5194/angeo-28-825-2010, 2010. 28166

5 Pal, S., Xueref-Remy, I., Ammoura, L., Chazette, P., Gibert, F., Royer, P., Dieudonné, E., Dupont, J.-C., Haeffelin, M., Lac, C., Lopez, M., Morille, Y., and Ravetta, F.: Spatio-temporal variability of the atmospheric boundary layer depth over Paris agglomeration: an assessment of the impact of urban heat island intensity, *Atmos. Environ.*, 63, 261–275, doi:10.1016/j.atmosenv.2012.09.046, 2012. 28159, 28162, 28165, 28186

10 Pérez-Landa, G., Ciais, P., Gangoiti, G., Palau, J. L., Carrara, A., Gioli, B., Miglietta, F., Schumacher, M., Millán, M. M., and Sanz, M. J.: Mesoscale circulations over complex terrain in the Valencia coastal region, Spain – Part 2: Modeling CO₂ transport using idealized surface fluxes, *Atmos. Chem. Phys.*, 7, 1851–1868, doi:10.5194/acp-7-1851-2007, 2007. 28159

Pergaud, J., Masson, V., Malardel, S., and Couvreur, F.: A parameterization of dry thermals and shallow cumuli for mesoscale numerical weather prediction., *Bound.-Layer Meteor.*, 132, 83–106, 2009. 28181

15 Pinty, J. and Jabouille, P.: A mixed-phased cloud parameterizations for use in a mesoscale non-hydrostatic model: simulations of a squall line and of orographic precipitation, in: *Conf. on Cloud Physics*, 217–220, Amer. Meteor. Soc., Everett, WA, 1998. 28181

20 Rödenbeck, C., Houweling, S., Gloor, M., and Heimann, M.: CO₂ flux history 1982–2001 inferred from atmospheric data using a global inversion of atmospheric transport, *Atmos. Chem. Phys.*, 3, 1919–1964, doi:10.5194/acp-3-1919-2003, 2003. 28158

Sarrat, C., Noilhan, J., Dolman, A. J., Gerbig, C., Ahmadov, R., Tolk, L. F., Meesters, A. G. C. A., Hutjes, R. W. A., Ter Maat, H. W., Pérez-Landa, G., and Donier, S.: Atmospheric CO₂ modeling at the regional scale: an intercomparison of 5 meso-scale atmospheric models, *Biogeosciences*, 4, 1115–1126, doi:10.5194/bg-4-1115-2007, 2007a. 28159, 28160

25 Sarrat, C., Noilhan, J., Lacarrère, P., Donier, S., Lac, C., Calvet, J.-C., Dolman, H., Gerbig, C., Neininger, B., Ciais, P., Paris, J. D., Boumard, F., Ramonet, M., and Butet, A.: Atmospheric CO₂ modeling at the regional scale: application to the CarboEurope regional experiment, *J. Geophys. Res.*, 112, D12105, doi:10.1029/2006JD008107, 2007b. 28158, 28160

30 Sarrat, C., Noilhan, J., Lacarrère, P., Masson, V., Ceschia, E., Ciais, P., Dolman, A., Elbers, J., Gerbig, C., and Jarosz, N.: CO₂ budgeting at the regional scale using a Lagrangian experimental strategy and meso-scale modeling, *Biogeosciences*, 6, 113–127, doi:10.5194/bg-6-113-2009, 2009. 28160

**CO₂ dispersion
modelling over Paris**

C. Lac et al.

[Title Page](#)[Abstract](#)[Introduction](#)[Conclusions](#)[References](#)[Tables](#)[Figures](#)[I◀](#)[▶I](#)[◀](#)[▶](#)[Back](#)[Close](#)[Full Screen / Esc](#)[Printer-friendly Version](#)[Interactive Discussion](#)

Seibert, P., Beyrich, F., Gryning, S. E., Joffre, S., Rasmussen, A., and Tercier, P.: Review and intercomparison of operational methods for the determination of the mixing height, *Atmos. Environ.*, 34, 1001–1027, 2000. 28158, 28166

Seity, Y., Brousseau, P., Malardel, S., Hello, G., Bénard, P., Bouttier, F., Lac, C., and Masson, V.: The AROME-France Convective-Scale Operational Model, *Mon. Weather Rev.*, 139, 976–991, 2010. 28161

Steenefeld, G., Mauritsen, T., Bruijn, E. D., de Arellano, J. V.-G., Svensson, G., and Holtslag, A.: Evaluation of limited-area models for the representation of the diurnal cycle and contrasting nights in CASES-99, *J. Appl. Meteor. Clim.*, 47, 869–887, doi:10.1175/2007JAMC1702.1, 2008. 28166

Takahashi, T., Feely, R. A., Weiss, R. F., Wanninkhof, R. H., Chipman, D. W., Sutherland, S. C., and Takahashi, T. T.: Global air-sea flux of CO₂: An estimate based on measurements of sea air CO₂ difference, *Proc. Natl. Acad. Sci. USA*, 94, 8292–8299, doi:10.1073/pnas.94.16.8292, 1997. 28161

Vautard, R., Menut, L., Beekmann, M., Chazette, P., Flamant, P. H., Gombert, D., Guedalia, D., Kley, D., Lefebvre, M. P., Martin, D., Megie, G., Perros, P., and Toupance, G.: A synthesis of the air pollution over the paris region (ESQUIF) field campaign, *J. Geophys. Res.*, 108, 8558, doi:10.1029/2003JD003380, 2003. 28157

Xueref-Remy, I., Pal, S., Lopez, M., Schmidt, M., Dieudonné, E., Vuillemin, C., Darding, M., and Wastine, B.: Atmospheric investigation of the role of the different emission sectors in the total CO₂ emission plume from the Paris megacity, *Geophys. Res. Abstr.*, 14, EGU2012–13419, 2012. 28157

**CO₂ dispersion
modelling over Paris**

C. Lac et al.

Table 1. Dynamical and physical options used in the Meso-NH model.

Vertical coordinates	Gal-Chen and Somerville
Basic equations	Non-hydrostatic, anelastic
Grid type	Arakawa C-grid
Transport schemes	WENO 3rd order for momentum PPM for meteorological and scalar variables
Time integration	2nd order Runge-Kutta split-explicit
Time step	60 s for the physics 15 s for the advection
Radiation	ECMWF scheme: Rapid Radiative Transfer Model Longwave and Fouquart Shortwave
Microphysics	Single moment class 5 (Pinty and Jabouille, 1998)
Turbulence	1-D Cuxart et al. (2000) with Bougeault and Lacarrere (1989) mixing length
Shallow convection	Eddy-Diffusivity Mass-Flux scheme (Pergaud et al., 2009)

[Title Page](#)[Abstract](#)[Introduction](#)[Conclusions](#)[References](#)[Tables](#)[Figures](#)[◀](#)[▶](#)[◀](#)[▶](#)[Back](#)[Close](#)[Full Screen / Esc](#)[Printer-friendly Version](#)[Interactive Discussion](#)

**CO₂ dispersion
modelling over Paris**

C. Lac et al.

Table 2. Mean observed, and Bias and Rmse of the BLH for the REF and RUR simulations. Nighttime is considered from 19:00 UT to 08:00 UT.

JUSSIEU				
	Mean Day		Mean Night	
OBS	867		222	
Simul	Bias Day	Rmse Day	Bias Night	Rmse Night
REF	−122	244	−47	67
RUR	−233	314	−92	108
SIRTA				
	Mean Day		Mean Night	
OBS	731		155	
Simul	Bias Day	Rmse Day	Bias Night	Rmse Night
REF	−86	326	−34	96
RUR	−179	389	−57	109
TRN				
	Mean Day			
OBS	661			
Simul	Bias Day	Rmse day		
REF	−85	355		
RUR	−105	319		

[Title Page](#)[Abstract](#)[Introduction](#)[Conclusions](#)[References](#)[Tables](#)[Figures](#)[I◀](#)[▶I](#)[◀](#)[▶](#)[Back](#)[Close](#)[Full Screen / Esc](#)[Printer-friendly Version](#)[Interactive Discussion](#)

CO₂ dispersion modelling over Paris

C. Lac et al.

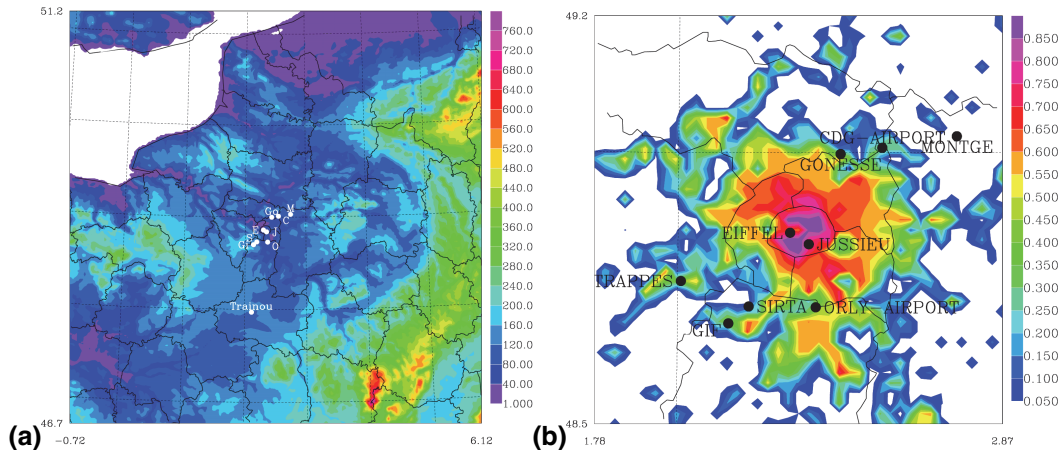


Fig. 1. (a): Domain of simulation with orography (in m a.s.l.). (b): Zoomed-in-view on Ile-de-France province with urban fraction. The observational stations (Montge, Gonesse, Eiffel, Jussieu, Trappes, SIRT A, Gif) and airports (CDG and Orly) are labelled on both panels.

Title Page

Abstract

Introduction

Conclusions

References

Tables

Figures

◀

▶

◀

▶

Back

Close

Full Screen / Esc

Printer-friendly Version

Interactive Discussion



CO₂ dispersion
modelling over Paris

C. Lac et al.

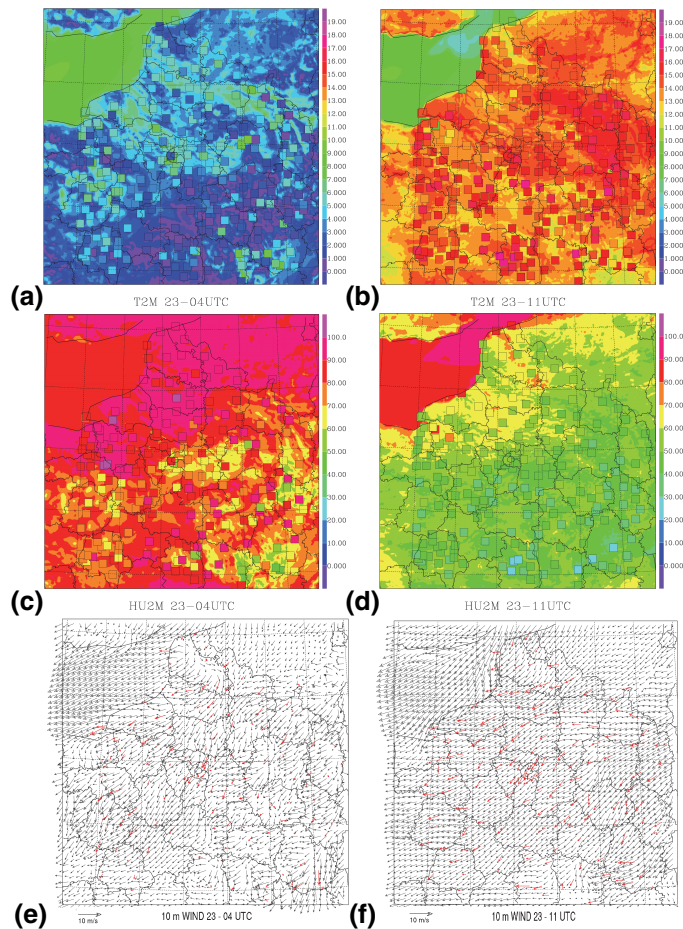


Fig. 2. MESO-NH predictions for 2 m relative temperature (in °C) (a and b), 2 m relative humidity (in %) (c and d) and 10 m wind (e and f) with observations shown by coloured squares/arrows for 23 March at 04:00 UT (on the left) and 11:00 UT (on the right).

Title Page

Abstract

Introduction

Conclusions

References

Tables

Figures

◀

▶

◀

▶

Back

Close

Full Screen / Esc

Printer-friendly Version

Interactive Discussion



CO₂ dispersion
modelling over Paris

C. Lac et al.

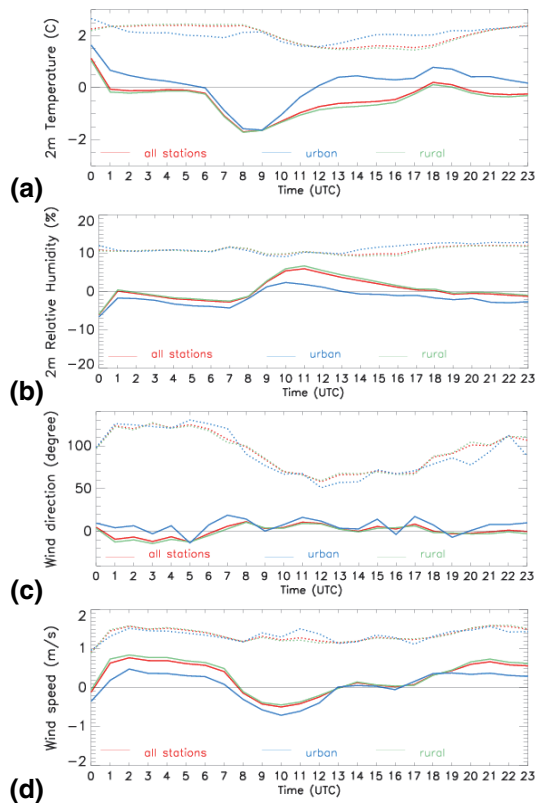


Fig. 3. Daily variation of the bias (solid line) and rmse (dashed line) for the REF simulations for the 2 m temperature (a), 2 m relative humidity (b), 10 m wind speed (c) and direction (d), considering all the stations (in blue), or decomposed between urban (in red) and rural stations (in green). Urban stations represent 35 stations over 235 stations for T2M, 33 stations over 182 stations for HU2M and 27 stations over 113 stations for the 10 m wind fields.

Title Page

Abstract

Introduction

Conclusions

References

Tables

Figures

◀

▶

◀

▶

Back

Close

Full Screen / Esc

Printer-friendly Version

Interactive Discussion



CO₂ dispersion
modelling over Paris

C. Lac et al.

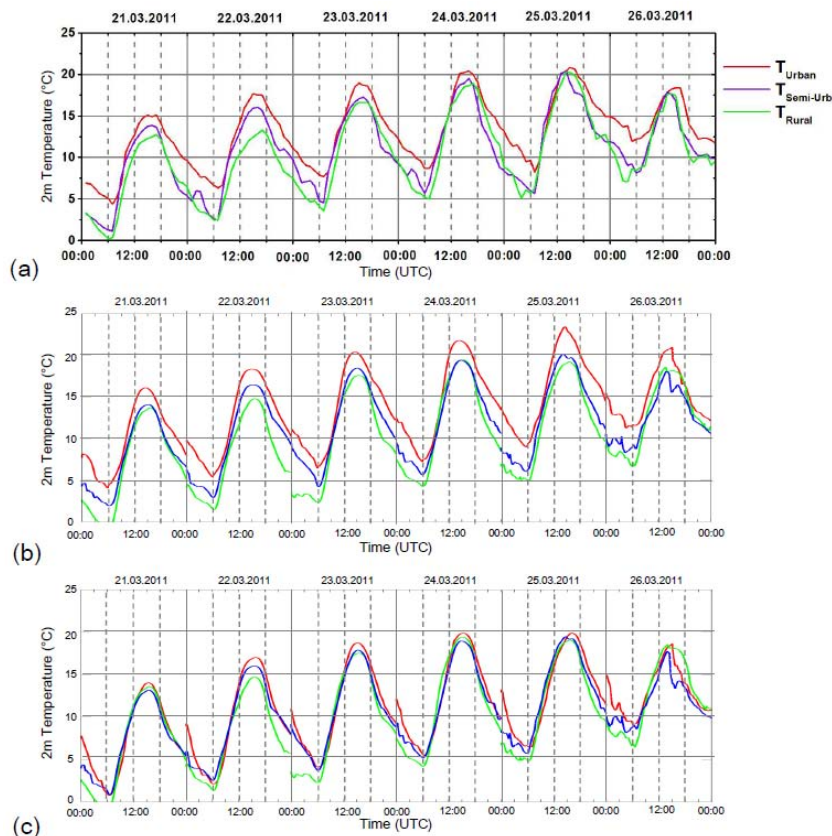


Fig. 4. Diurnal variation of hourly near surface air temperature (in °C) at urban, sub-urban and rural stations measured (from Pal et al., 2012) **(a)**, predicted with REF simulations **(b)** and RUR simulations **(c)**.

[Title Page](#)[Abstract](#)[Introduction](#)[Conclusions](#)[References](#)[Tables](#)[Figures](#)[◀](#)[▶](#)[◀](#)[▶](#)[Back](#)[Close](#)[Full Screen / Esc](#)[Printer-friendly Version](#)[Interactive Discussion](#)

CO₂ dispersion
modelling over Paris

C. Lac et al.

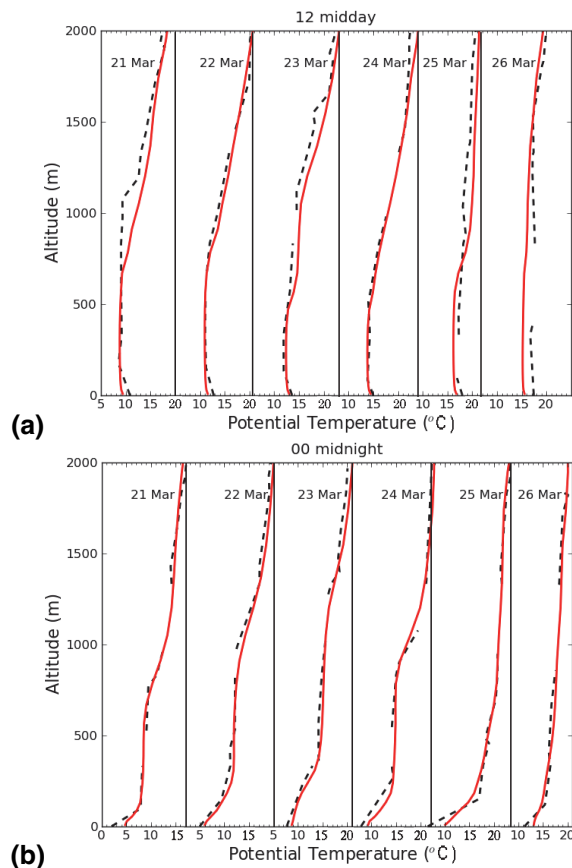


Fig. 5. Vertical profiles of potential temperature (in °C) above the Trappes location for 12:00 UT **(a)** and 00:00 UT **(b)** for the measurements (black dashed lines) and REF simulations (solid red lines).

[Title Page](#)[Abstract](#)[Introduction](#)[Conclusions](#)[References](#)[Tables](#)[Figures](#)[◀](#)[▶](#)[◀](#)[▶](#)[Back](#)[Close](#)[Full Screen / Esc](#)[Printer-friendly Version](#)[Interactive Discussion](#)

CO₂ dispersion
modelling over Paris

C. Lac et al.

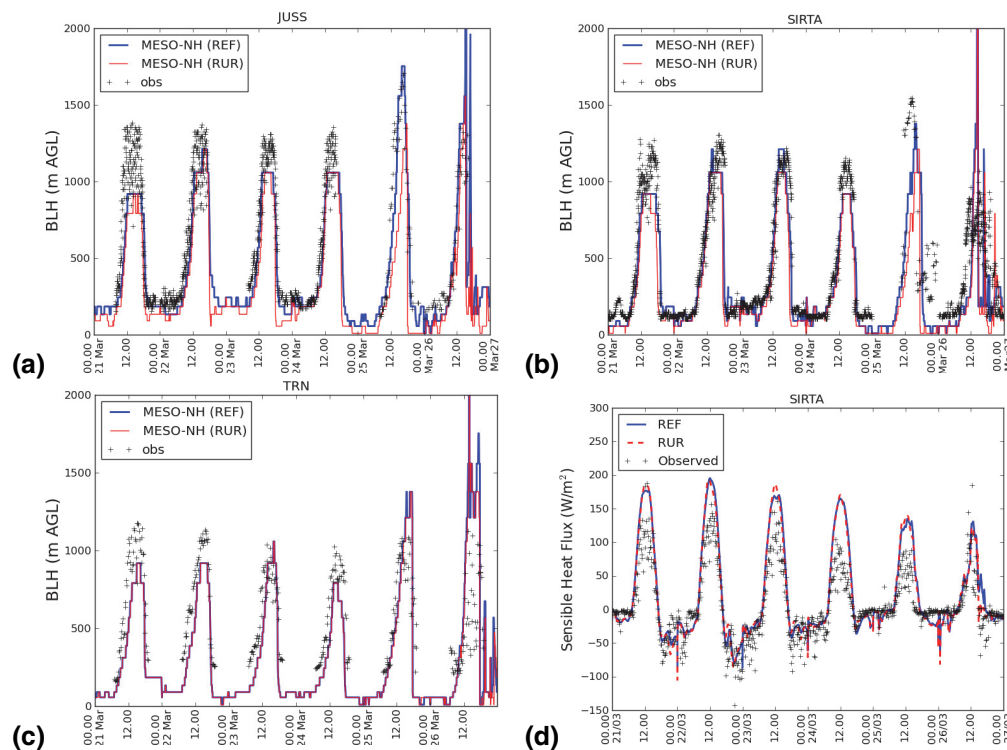


Fig. 6. Time series of BLH (in meters a.g.l. (AGL)) for 21–26 March at JUSS (a, urban site), SIRTA (b, sub-urban site) and TRN (c, rural site) and sensible heat fluxes (in $W\ m^{-2}$) at SIRTA site (d).

Title Page

Abstract

Introduction

Conclusions

References

Tables

Figures

◀

▶

◀

▶

Back

Close

Full Screen / Esc

Printer-friendly Version

Interactive Discussion



CO₂ dispersion
modelling over Paris

C. Lac et al.

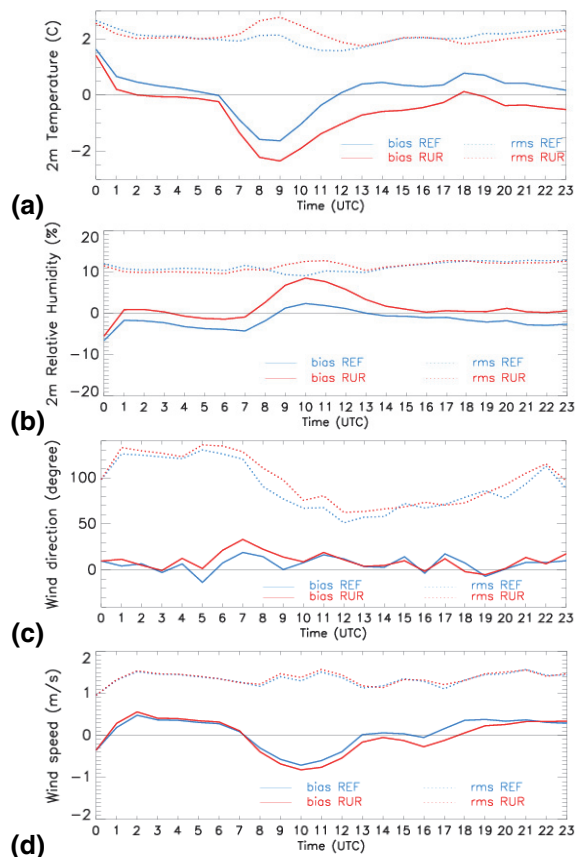


Fig. 7. Daily variation of the bias (solid line) and rmse (dashed line) for the REF (in blue) and RUR simulations (in red) for the 2 m temperature **(a)**, 2 m relative humidity **(b)**, 10 m wind speed **(c)** and 10 m wind direction **(d)** only for the urban stations.

Title Page

Abstract

Introduction

Conclusions

References

Tables

Figures

◀

▶

◀

▶

Back

Close

Full Screen / Esc

Printer-friendly Version

Interactive Discussion



CO₂ dispersion
modelling over Paris

C. Lac et al.

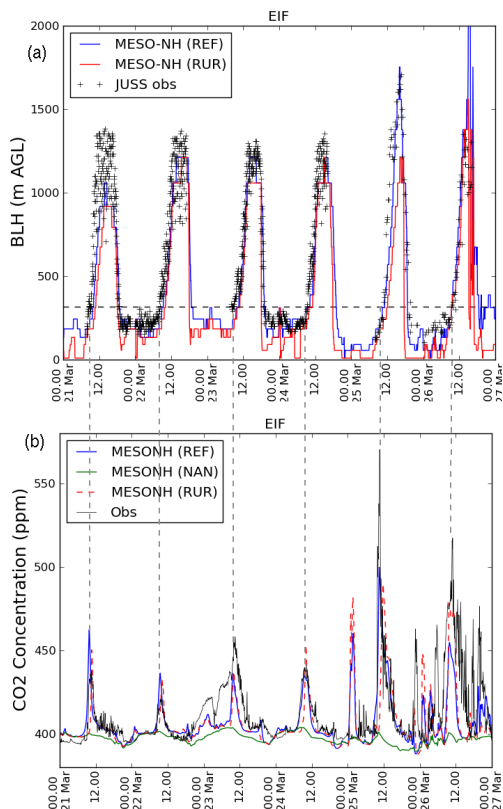


Fig. 8. (a) Time series of BLH predictions at Eiffel and observations at JUSS (in m a.g.l., AGL) for REF (blue) and RUR (red) simulations. (b) Time series of CO₂ predictions and observations (in ppm) at EIF for REF (blue), RUR (red) and NAN (green) simulations. The vertical dashed lines correspond to the time in the morning at which observed BLHs reach 310 m (Eiffel measurement height).

Title Page

Abstract

Introduction

Conclusions

References

Tables

Figures

◀

▶

◀

▶

Back

Close

Full Screen / Esc

Printer-friendly Version

Interactive Discussion



CO₂ dispersion
modelling over Paris

C. Lac et al.

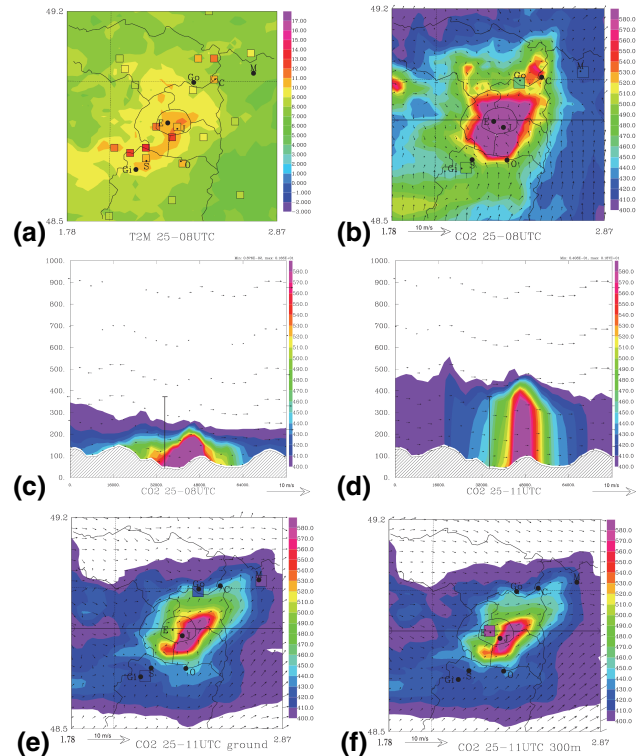


Fig. 9. MESO-NH predictions: for 25 March at 08:00 UT (a) 2 m temperature (in °C), (b) Horizontal cross section of CO₂ concentration (in ppm) near the ground. (c) Vertical cross section of CO₂ concentration (in ppm) according to the axis given in (b) for 25 March at 08:00 UT, and for 25 March at 11:00 UT (d), with wind vectors superimposed. The Eiffel tower is symbolized by a stick, with a length corresponding to its measurement height. Horizontal ticks indicate meters. For 25 March at 11:00 UT: Horizontal cross-section of CO₂ concentration (in ppm) near the ground (e) and at 300 m height (f) with wind arrows superimposed. Coloured squares mean observed CO₂ concentration.

Title Page

Abstract

Introduction

Conclusions

References

Tables

Figures

◀

▶

◀

▶

Back

Close

Full Screen / Esc

Printer-friendly Version

Interactive Discussion



CO₂ dispersion
modelling over Paris

C. Lac et al.

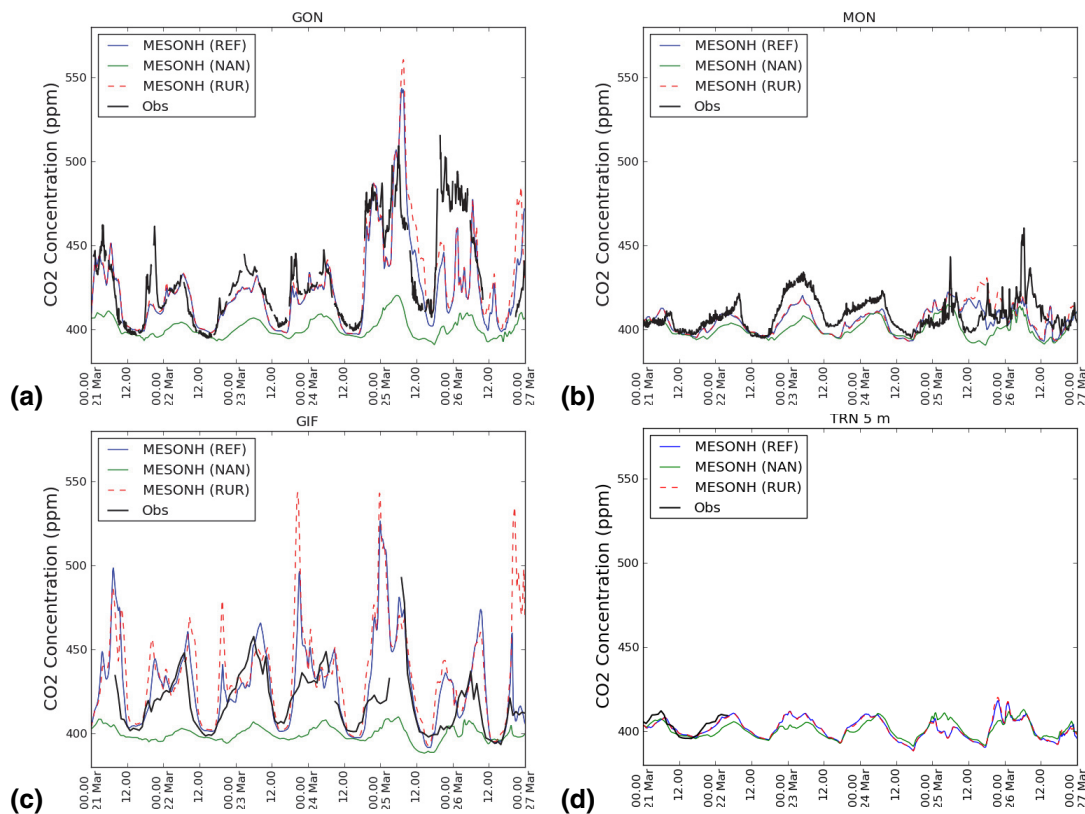


Fig. 10. Temporal evolution of CO₂ concentrations (in ppm) measured (black line) and predicted with REF (blue line), RUR (red line) and NAN (green line) simulations at Gonesse **(a)**, Montge-en-Goelle **(b)**, Gif-sur-Yvette **(c)** and Trainou **(d)**.

Title Page

Abstract

Introduction

Conclusions

References

Tables

Figures

◀

▶

◀

▶

Back

Close

Full Screen / Esc

Printer-friendly Version

Interactive Discussion



CO₂ dispersion modelling over Paris

C. Lac et al.

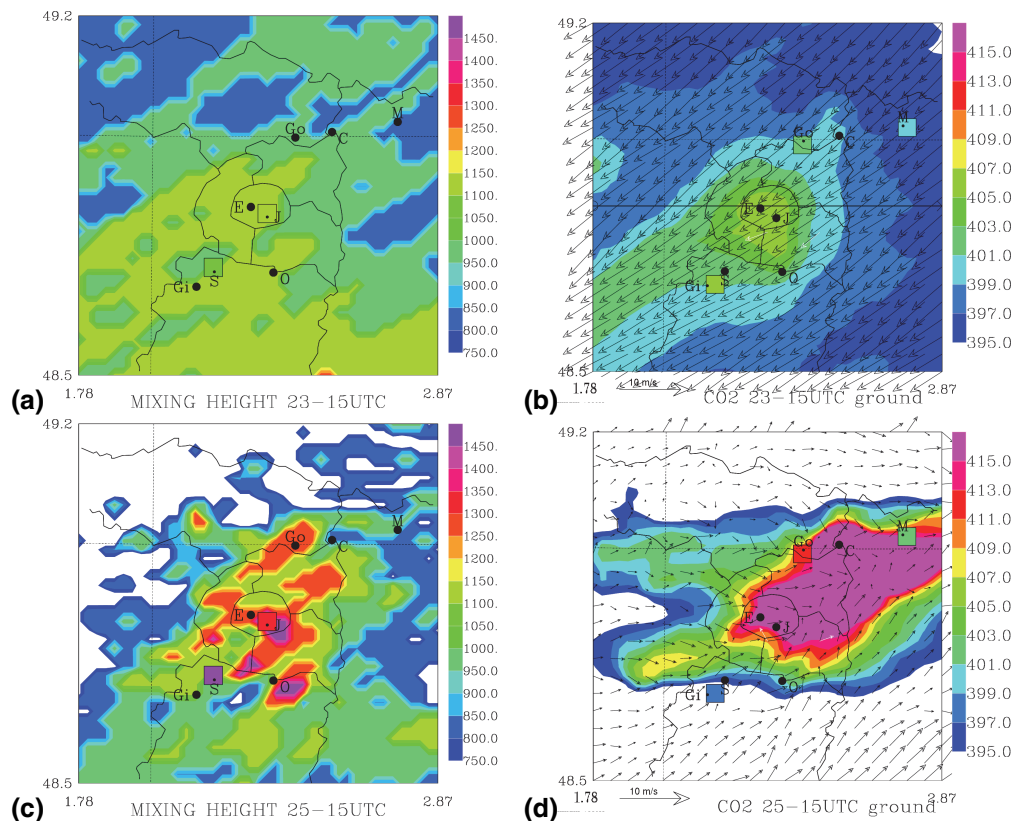


Fig. 11. MESO-NH predictions for 23 March at 15:00 UT (on the upper part) and for 25 March at 15:00 UT (on the lower part) of BLH (in m a.g.l.) (on the left) and CO₂ concentration (in ppm) near the ground (on the right). Observations for both fields are added in coloured squares, and predicted wind arrows (in ms⁻¹) on CO₂ concentration. White colours correspond to values less than the minimum coloured one.

Title Page

Abstract Introduction

Conclusions References

Tables Figures

◀ ▶

◀ ▶

Back Close

Full Screen / Esc

Printer-friendly Version

Interactive Discussion

